

Heat and mass transfer characteristics of a rotating regenerative total energy wheel

Ephraim M. Sparrow^{a,*}, Jimmy C.K. Tong^a, Mark R. Johnson^a, Gerry P. Martin^b

^a *Laboratory for Heat Transfer Practice, Department of Mechanical Engineering, University of Minnesota,
111 Church Street S.E., Minneapolis, MN 55455, USA*

^b *Air Energy Research Corporation, Minneapolis, MN 55406, USA*

Received 25 May 2006; received in revised form 29 July 2006

Available online 26 January 2007

Abstract

An experimental investigation has been carried out to determine the operating performance of a rotating regenerative total energy wheel (TEW). A total energy wheel is a device which conserves both sensible and latent energies. It transfers heat from a warmer to a cooler airstream while simultaneously transferring moisture from a more humid to a less humid airstream. The effectiveness of a TEW device has been measured in a special experimental facility which incorporates features that enable the obtainment of data of high accuracy. The heart of the facility is a spacious, compartmented plenum chamber made from extruded, closed-cell polystyrene which is free of extraneous heat transfer and air leakage. The plenum allows for well-defined inlet and exit conditions for the heat/moisture exchanger being evaluated. Only the plenum need be reconfigured to accommodate each heat/moisture exchanger type, a task that can be performed in a day. The remainder of the facility is universal for all heat/moisture exchangers. Most of the instrumentation is located in the universal part of the facility and is not affected by plenum reconfigurations.

© 2006 Published by Elsevier Ltd.

Keywords: Total energy wheel; Heat exchanger; Moisture exchanger; Test facility; Instrumentation

1. Introduction

In the continuing effort to achieve comfort control while diminishing the power required to fulfill comfort standards, the *total energy wheel* (TEW) is gaining considerable prominence. The special feature that makes the TEW attractive is that it is able to serve as a means for control of both temperature and humidity. A schematic representation of a TEW is presented in Fig. 1. As seen there, an air-permeable rotating disk is situated in a ductwork system consisting of a pair of rectangular ducts. The upper half of the disk is fed by air moving from right to left through the upper duct, while the lower half of the disk is fed by air flow from left to right through the other duct. The two air streams pass

through the disk in counter flow. Downstream of the disk, each of the ducts continues and serves to collect the respective air streams that exit the disk.

The disk consists of an assemblage of a large number of parallel flow passages. Although many shapes of flow-passage cross sections are possible, the most common passage cross section is a trapezoid as can be seen in the photograph of Fig. 2. In most cases, the walls of the flow passages are metallic, but plastics have also been used for limited service.

One of the two air streams may be regarded as hot and humid; for example, air coming from the outdoors on a hot, mid-summer day in a moist climate. The other stream would then be that which is the exhausted from an indoor conditioned space to fulfill an air exchange code or to satisfy air quality needs. That exhaust air would have a moderate temperature and moderate humidity. The function of the TEW is to diminish both the temperature and humidity

* Corresponding author. Tel.: +1 612 625 5502.
E-mail address: esparrow@umn.edu (E.M. Sparrow).

Nomenclature

\dot{m}_{Return}	mass flowrate of the return airstream
$\dot{m}_{\text{Return,dryair}}$	mass flowrate of dry air in the return airstream
\dot{m}_{Supply}	mass flowrate of the supply airstream
$\dot{m}_{\text{Supply,dryair}}$	mass flowrate of dry air in the supply airstream
T_{Intake}	temperature of the intake airstream
T_{Return}	temperature of the return airstream
T_{Supply}	temperature of the supply airstream

Greek symbols

ε	sensible heat effectiveness
$\varepsilon_{\text{moisture}}$	latent effectiveness
ω_{Intake}	humidity ratio of the intake airstream
ω_{Return}	humidity ratio of the return airstream
ω_{Supply}	humidity ratio of the supply airstream

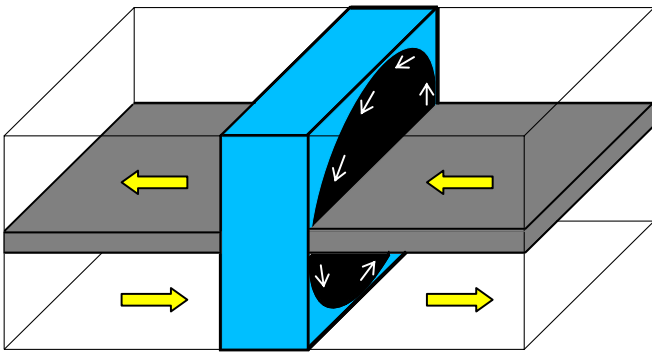


Fig. 1. Schematic diagram of an installed total energy wheel.



Fig. 2. Photograph of a portion of a total energy wheel showing the trapezoidal cross sections of the flow passages.

in the air that is drawn from the outdoors en route to the conditioned space in order to replace that which is being exhausted. The means by which the TEW accomplishes this goal is to absorb both heat and moisture from the hot, humid air stream and to unload the heat and moisture into the cooler, drier air stream. The absorption process is accomplished as the disk rotates slowly through the upper half of its circular path, while the unloading occurs as the disk moves through the lower half of its path.

Heat absorption naturally occurs because the structural material that bounds the flow passages has heat capacity and absorbs heat whenever the temperature of the passage wall is lower than that of the airflow. On the other hand, in order that moisture be absorbed/adsorbed on the walls of the flow passages, a hydrophilic coating (desiccant) must be applied to the walls. There are a number of generic types of coatings that can serve this purpose, including molecular sieves and gels. However, the specific coatings that are used commercially are generally proprietary.

Total energy wheels are commercially available through a number of manufacturers and vendors, and each manufacturer typically provides performance information. On the other hand, according to a thorough literature search performed by the authors, there appears to be no open-literature experimental information for realistic TEWs. An early experimental paper [1] dealt with a wheel having uncoated flow passages, a situation which precludes moisture transfer. More recently, experiments with coated flow passages were reported [2] for a unique configuration in which only a quarter of the face area of the rotating disk was exposed to each of the air streams. In contrast, the literature contains a considerable number of numerical simulations, ranging from a first publication in 1970 [3] to a latest publication in 1999 [4].

With the expected increased use of TEWs in the forthcoming years, there is a need to create a testing methodology for obtaining performance information of consistently high accuracy. This paper sets forth the underlining principles and the physical implementation of a test facility capable of providing performance data of impeccable quality. The facility is described in detail, including instrumentation and data acquisition means. To illustrate the practical utility of the facility, experiments encompassing both heat and moisture transfer will be reported for a representative TEW. Effects of cross-channel leakage will also be identified.

2. The test facility

The underling principles that guided the design and fabrication of the test facility included: (a) the avoidance of extraneous heat losses/gains, air leakage, and moisture

leakage, (b) attainment of well-defined velocity, temperature, and water vapor profiles at all measurement stations, (c) operation in the suction mode to achieve greater uniformity of the flow delivered to the test facility, (d) use of spacious plenum chambers both upstream and downstream of the total energy wheel to establish well-defined inlet conditions, and (e) use of highly accurate instrumentation supplemented with redundancy.

An overall schematic diagram displaying the general features of the test facility is presented in Fig. 3. Its description is facilitated by following the pathway of the fluid flow of each of the individual participating streams. At the lower left is an opening into which is drawn air from the laboratory room. That air stream is designated as the *return stream*. The return stream passes through a length of large-diameter round pipe, the exit of which discharges the air into a large rectangular plenum chamber (see Fig. 4). The plenum serves to homogenize the flow prior to its encounter with the rotating wheel. This plenum delivers air to the lower half of the wheel. Downstream of the wheel, there is a second plenum chamber which is directly in line with the aforementioned upstream plenum. That plenum receives the air that exits the lower half of the wheel. At the downstream end of the second plenum is a connection to another large-diameter round pipe which is termed the exhaust pipe because it carries the *exhaust stream* to the outdoors. At the end of the exhaust pipe is situated a blower that is operated in the suction mode.

The second air stream is drawn into the test facility from the outdoors via a round pipe identical to the others. That incoming stream is called the *intake stream*. This stream is delivered to a third plenum chamber that is identical in every way to those mentioned in the preceding paragraph. The air passing through this plenum is fed to the upper half of the rotating wheel. The air exiting the upper half of the wheel passes into a fourth plenum chamber that is in line with the third plenum. The downstream end of the fourth plenum mates with another large-diameter round pipe. In a normal field installation, the air stream passing through the latter pipe would exit into a space to be conditioned, and that stream would be designated as the *supply stream*. However, in the present test facility, where the suction mode is a key design feature, the supply stream is ducted through a pair of right-angle bends and, thereafter, through a long straight pipe to its exit outdoors. A blower operating in a suction mode is positioned at the exit.

A key feature of the plenum chambers is their material of construction. The walls of the plenums are made from 38-mm-thick (1.5 in.) extruded, closed-cell polystyrene. The selection of polystyrene as the plenum wall material was based on its outstanding insulating properties, with a corresponding negligible heat loss/gain as estimated by calculation. The polystyrene sheets were assembled in a manner to guarantee the absence of air and moisture leakage. To this end, all mating polystyrene surfaces were coated with an impermeable caulk prior to the assembly. The

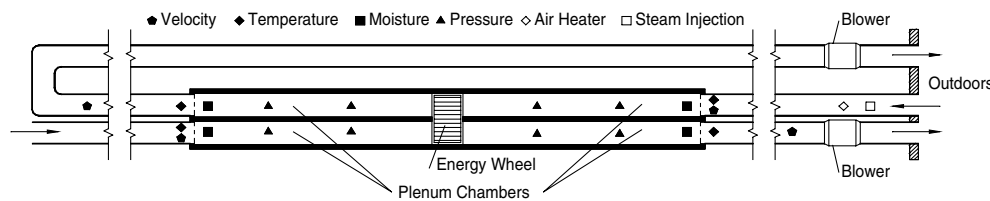


Fig. 3. Overall schematic of the test facility.

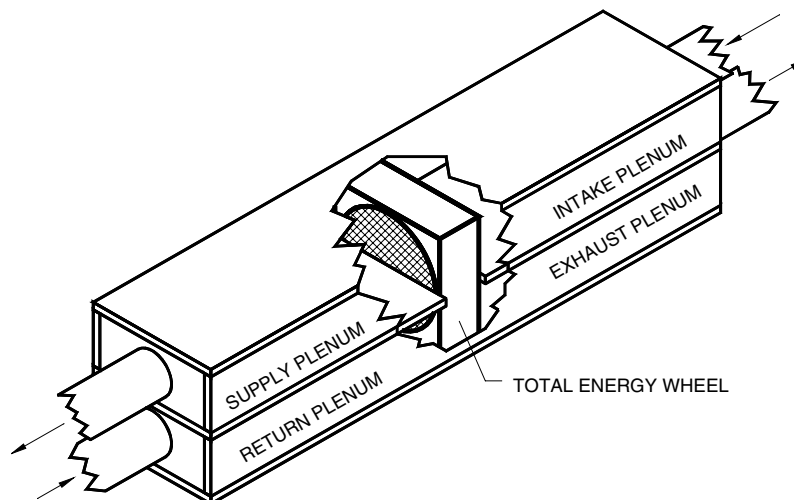


Fig. 4. Detailed depiction of the plenum chambers and the total energy wheel.

structural integration of the sheets was accomplished by the use of very long wood screws mating with plastic inserts of the type used to anchor screws in concrete walls. This mode of attachment resulted in an extremely rigid structure without gaps between the mating sheets. To verify the leak-free nature of the final construction, the plenum chambers were pressurized and all joints were carefully evaluated using the soap-bubble technique. All polystyrene–metal and metal–metal interfaces were multiple caulked and carefully evaluated under pressurization.

As a further precaution against heat losses/gains, all of the large-diameter metallic pipes were painstakingly wrapped with fiberglass insulation which, in turn, was wrapped with aluminum-foil sheets.

Attention will now be turned to the instrumentation that was installed in the test facility. The quantities whose values are essential to the evaluation of the performance of the tested object (for example, a TEW) are (a) the temperatures of the intake, supply, return, and exhaust airstreams, (b) the moisture content (humidity) of the respective four airstreams, (c) the mass flowrates of dry air in the four individual streams, (d) the mass flowrates of moisture in the four individual streams, and (e) pressures in each of the four plenum chambers. Among these quantities, temperatures, humidities, and pressures were measured directly, while the other quantities were calculated from these measurements and the measurements of velocity profiles.

With regard to temperature, two traversing thermocouples were installed at each of the measurement locations depicted in Fig. 3. Complete cross-sectional traverses were made at each measurement location, and the relationship between the average temperature and the maximum temperature in each cross section was established. A similar procedure was performed with regard to the velocity. In particular, complete traverses at each velocity measurement site yielded the ratio of the maximum to the mean velocity. In subsequent uses of the facility, measurements were made only of the maximum temperatures and velocities at the respective sites. These values were then converted to the corresponding mean values. In the case of velocity, the respective mean velocities were multiplied by the corresponding cross-sectional area to yield the volumetric flowrates. When the respective volumetric flowrates were multiplied by the corresponding densities of the moist and dry air, the mass flowrates were determined.

The velocity measurements were performed with a Pitot tube in conjunction with a micromanometer which could be read to 0.001 in. of water column. For the temperature measurements, the thermocouple emfs were collected by a data logger which was connected to a computer. The calibrated accuracy of the thermocouples was 0.1 °F.

At each of the designated humidity measurement locations, a small-diameter plastic tube was installed which spanned the entire cross section. In each of the tubes, a series of small holes was drilled along the length of the tube. These holes served as sampling ports. A slight suction was applied to each of the tubes to maintain a continuous

intake of the moist air. The samples of air from each measurement site were ducted to a humidity measuring station. Each station consisted of a wet-bulb and a dry-bulb thermocouple. For the wet-bulb thermocouple, a continuous supply of water was provided to ensure that the sensing tip was always properly wetted. The emfs from each of the thermocouples were electronically collected and conveyed to a computer for further processing.

The humidity measurements enabled the determination of the humidity ratio at each site. The knowledge of the humidity ratio facilitated the measured flowrate of the moist air to be subdivided into a dry-air flowrate and a moisture flowrate.

The pressures in the respective plenum chambers were measured with a view toward detecting possible air leakage between the plenums. The actual pressures were read with the aid of a micromanometer.

3. Representative results

A measure of the performance of the test facility can be obtained by comparing the rates of fluid inflow into the facility and fluid outflow from the facility. Such a comparison is often called a mass balance. In the present situation, where the flowing fluid is humid air, it is appropriate to look at separate mass balances for the flow of dry air and for the flow of moisture. Table 1 conveys representative mass-balance results for a number of experimental conditions. In the table, separate comparisons are made for dry air and moisture. For the dry air, the balance between inflow and outflow is fulfilled to within 2–3%. A similar comparison for the moisture flow also yields a balance in the same range. The excellence of the mass balances provides strong testimony to the tightness of the test facility with regard to leakage between the inside of the facility and the surrounding environment.

As an illustration of the nature of the results that can be obtained from the test facility, experiments were performed involving a total energy wheel installed as pictured in Fig. 3. The characteristics of the TEW that was tested are

- (a) Outer diameter of the wheel = 61 cm (24 in.); hub diameter = 20.3 cm (8 in.)
- (b) Streamwise length of the wheel = 25.4 cm (10 in.)
- (c) Number of flow passages = ~100,000

Table 1
Representative mass-balance results

Run no.	Dry airflow		Moisture flow	
	In (kg/min)	Out (kg/min)	In (kg/min)	Out (kg/min)
1	19.28	19.60	0.22	0.22
2	37.69	38.51	0.37	0.38
3	53.16	53.89	0.79	0.81
4	61.55	63.41	0.73	0.74

(d) Cross-sectional area of a flow passage = 0.0142 cm² (0.0022 in.²)

Each flow passage had a sine-wave cross section. As operated during the experiments, there was no purge section. All the experiments were performed at the rotational speed of 20 rpm.

To demonstrate the results, Figs. 5 and 6 have been prepared. The first of these figures presents information for the *sensible heat effectiveness* ϵ . This effectiveness is used to characterize the heat transfer performance of heat exchangers in general. It is defined as

$$\epsilon = \frac{\dot{m}_{\text{Supply}}(T_{\text{Supply}} - T_{\text{Intake}})}{[\min(\dot{m}_{\text{Supply}}; \dot{m}_{\text{Return}})](T_{\text{Return}} - T_{\text{Intake}})} \quad (1)$$

In this equation, \dot{m}_{Supply} is the rate of airflow passing through the wheel from the intake to the supply. In turn, \dot{m}_{Return} is the rate of airflow passing through from the return to the exhaust. The notation $\min(\dot{m}_{\text{Supply}}; \dot{m}_{\text{Return}})$ is used to identify the smaller of the two flowrates, \dot{m}_{Supply} and \dot{m}_{Return} . The temperatures appearing in Eq. (1) are those measured as described earlier.

Representative results for the sensible heat effectiveness have been plotted in Fig. 5. In the figure, the effectiveness is plotted as a function of the volumetric flowrate expressed

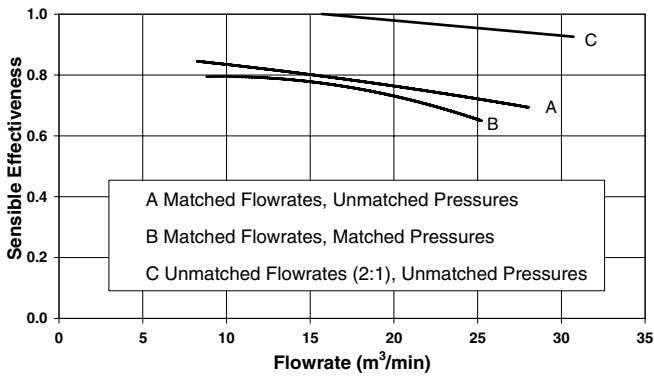


Fig. 5. Sensible heat effectiveness.

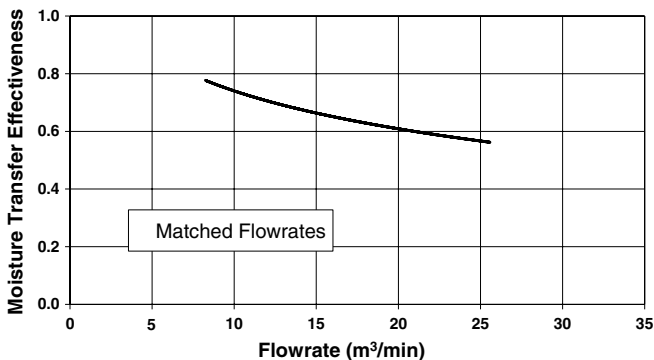


Fig. 6. Moisture transfer effectiveness.

as standard cubic meters per minute. Results for three different operating conditions are displayed in the figure. The first operating condition corresponds to matched mass flowrates of the intake-to-supply stream and the return-to-exhaust stream. For that situation, no attempt was made to match the pressures in the supply and the return plenum chambers. In the presence of unmatched pressures, air leakage between the two plenums might have occurred. If there was such leakage, it is likely to have occurred at the interface of the rotating wheel and non-rotating components. Although brush seals are positioned at that interface, the seal is necessarily imperfect. The second operating condition was similar to the first, except that the pressures in the supply and return plenums were matched. In the third case, the mass flowrate of the return-to-exhaust stream was twice that of the intake-to-supply stream. The pressures for that case were not matched.

In all cases, the sensible effectiveness displayed its characteristic decreases with increasing flowrate. For the matched flowrate cases, the issue of matched pressures was seen to play only a minor role. When the flowrates were unmatched, higher values of effectiveness were encountered, once again reinforcing available qualitative information.

An additional display of the capabilities of the test facility is conveyed in Fig. 6. In that figure, the *moisture transfer effectiveness* is plotted as a function of volumetric flowrate. In the published literature, the moisture transfer effectiveness is often designated as the *latent effectiveness*. The definition of the moisture transfer effectiveness is based on the humidity ratio ω . It is

$$\epsilon_{\text{moisture}} = \frac{\dot{m}_{\text{Supply,dryair}}(\omega_{\text{Intake}} - \omega_{\text{Supply}})}{[\min(\dot{m}_{\text{Supply,dryair}}; \dot{m}_{\text{Return,dryair}})](\omega_{\text{Intake}} - \omega_{\text{Return}})} \quad (2)$$

The data that are shown in Fig. 6 correspond to matched flowrates and to plenum pressures that are unmatched. Once again, the characteristic trend of the effectiveness decreasing with increasing flowrate is clearly in evidence. A comparison of Figs. 5 and 6 shows that the moisture transfer effectiveness is slightly lower than the sensible effectiveness.

4. Concluding remarks

This paper has presented the special features of a test facility capable of providing highly accurate data for air-to-air heat/moisture exchangers. Aside from the features that have already been described, there are others that are worthy of note. One is the low cost of the facility, both with regard to materials of construction and to the time required for fabrication. Low cost and simple fabrication are hallmarks of flexibility. This flexibility enables easy accommodation of the test facility to a wide variety of heat/moisture exchanger types and sizes.

The accommodation of the facility to any heat/moisture exchanger of interest is accomplished by either alteration or rebuilding of the plenum chambers. Since the plenums are made of extruded polystyrene, a complete rebuilding, if necessary, could be performed in a day.

Aside from the plenums, the remainder of the test facility is universal and would not require alteration to accommodate other heat/moisture exchangers. Furthermore, since the velocity and temperature instrumentation is located either upstream or downstream of the plenums, that instrumentation would not be affected if the plenums were to be rebuilt. Only the humidity sampling probes would have to be reinstalled.

The attributes of high accuracy, convenient operation, low cost, simple fabrication, and flexibility with regard to

the accommodation to many types of heat/moisture exchangers are the hallmarks of the present test facility.

References

- [1] J.G. van Leersum, C.W. Ambrose, Comparisons between experiments and a theoretical model of heat and mass transfer in rotary regenerators with nonsorbing matrices, *J. Heat Transfer* 103 (1981) 189–195.
- [2] C.J. Simonson, D.L. Ciepliski, R.W. Besant, Determining the performance of energy wheels: Part I - experimental and numerical methods, *ASHRAE Trans.* 105 (1999) 174–187.
- [3] R.V. Dunkle, I.L. Maclaine-cross, Theory and design of rotary regenerators for air conditioning, *Mech. Chem. Eng. Trans. Inst. Eng. Aust.* 6 (1970) 1–6.
- [4] C.J. Simonson, R.W. Besant, Energy wheel effectiveness: Part II – correlations, *Int. J. Heat Mass Transfer* 42 (1999) 2171–2185.